ACS Medicinal Chemistry Letters

Letter

Cite This: ACS Med. Chem. Lett. 2019, 10, 811−815

pubs.acs.org/acsmedchemlett

Design and Synthesis of Pyrrolidine-based Fragments That Sample Three-dimensional Molecular Space

Philip Garner,*[,†] Philip B. Cox,*[,¶] Upendra Rathnayake,[†] Nicholas Holloran,[†] and Paul Erdman[¶]

[†]Department of Chemistry, Washington State University, Pullman, Washington 99164-4630, United States

[¶]Discovery Chemistry and Technology, AbbVie Inc., 1 North Waukegan Road, North Chicago, Illinois 60064-6217, United States

Supporting Information

ABSTRACT: Fragment-based drug discovery (FBDD) is a well-established technology for lead compound generation in drug discovery. As this technology has evolved, the design of fragments for screening has also evolved to engender not just an understanding of the role of modulating the physicochemical properties of fragments (Rule of Three, Ro3) but also the importance and implications of incorporating shape and, in particular, 3D characteristics into fragments. Herein, we describe the design and synthesis of pyrrolidine-based fragments with good fragment-like (Ro3) physicochemical properties that effectively sample three-dimensional molecular space.

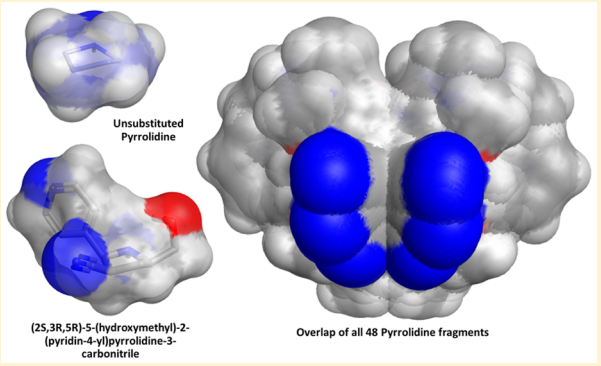

KEYWORDS: *Fragment design, functionalized pyrrolidines, asymmetric synthesis, molecular shape, 3D space*

Fragment-based drug discovery is a well-established front-line technology for the generation of high quality small molecule leads, clinical candidates and drugs.[1] The quest to identify fragments containing the correct balance of properties that enable efficient optimization is an ongoing goal for fragment-based lead discovery campaigns. On top of restricting molecular complexity (size) and balancing physicochemical properties (such as Rule of Three, Ro3), there has been significant interest in modulating properties via structural features that dictate the overall levels of saturation and shape of fragments. While there has been much debate over what exactly constitutes the correct level of saturation (defined in this Letter as Fsp^3 = fraction of sp^3 carbons/total number of carbons) and shape of fragments, there is agreement among practitioners that fragments should contain a balance of saturation/unsaturation and at least one aryl group. Such molecules will have sufficient levels of entropic and enthalpic contributions to target binding. In addition to saturation, molecular shape—and more specifically the three-dimensional (3D) character of fragments—is an area of significant interest and debate among the fragment community.[2] A properly designed fragment library will not only explore 3D pharmacophore space for hits but will also provide synthetic access to 3D functionalization space, which is desirable for hit-to-lead evolution. Saturation and 3D-character are also known to impart favorable physicochemical properties to fragments, in particular improved solubility.

In addition to the aforementioned design criteria, there is also significant interest in synthesizing fragments stereoselectively and creating homochiral fragment scaffolds with predefined chirality and therefore a proclivity toward enhanced 3D character. One fragment scaffold that is of particular interest in the fragment community is pyrrolidine. Apart from being a scaffold present in many natural products and drugs,[3] appropriately substituted pyrrolidines provide good coverage of functional vector space for fragment optimization. Furthermore, pyrrolidines can provide expanded 3D coverage via energetically accessible conformations that result from pseudorotation. To take advantage of these attributes, robust and flexible chemistries that strategically enable the synthesis of pyrrolidine fragments covering 3D molecular space are needed.

Metal-catalyzed asymmetric 1,3-dipolar cycloaddition of azomethine ylides and olefinic dipolarophiles provides a general route to diversely functionalized homochiral pyrrolidines.[4,5] Yet, despite the maturity of this reaction, examples using heteroaromatic Schiff bases to access the corresponding 2- (or 5-) heteroaromatic-substituted pyrrolidines are relatively rare.[6−15] One potential problem that could arise when using chiral ligands to control the developing stereochemistry is that the presence of Lewis-basic heteroatoms in the substrates may also form dative bonds with the metal, disrupting and/or competing with formation of the desired intermediate chiral ligand−metal−azomethine ylide complex. This competing ligand problem could become acute in instances where the heteroaromatic ring is capable of chelation with the imine

Received: February 22, 2019
Accepted: April 12, 2019
Published: April 12, 2019

DOI: 10.1021/acsmedchemlett.9b00070
ACS Med. Chem. Lett. 2019, 10, 811−815

nitrogen, with the exception of special cases where such chelation is, by design, integral to the complex structure. We reasoned that general access to homochiral heteroaromatic pyrrolidines might be achieved by using a chiral auxiliary attached to the azomethine ylide for stereocontrol rather than relying on chiral ligand mediated asymmetric induction.

The *endo*-selective[16] and *exo*-selective[17] asymmetric [C + NC + CC] cycloaddition reactions, originally developed to enable the transient generation and subsequent auxiliary-controlled 1,3-dipolar cycloaddition of azomethine ylides derived from enolizable aliphatic aldehydes, seemed well-suited to our purposes (Scheme 1). Synthesis of the

Scheme 1. Asymmetric [C + NC + CC] Cycloaddition-enabled Synthesis of a Pyrrolidine-based Fragment Library

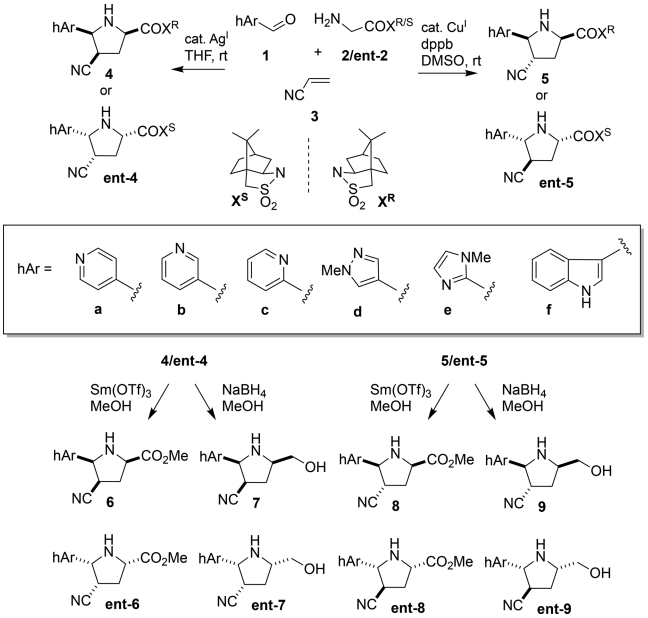

heteroaromatic pyrrolidine fragments was carried out in the following manner: the Ag(I)-catalyzed *endo*-selective [C + NC + CC] reaction proceeded through a Schiff base formed by the condensation of aldehyde **1** and glycylsultam **2**/**ent-2**, followed by generation of a metallo-azomethine ylide that reacts with the dipolarophile **3** in a concerted manner to give the *endo*-cycloadducts **4**/**ent-4**. However, the complementary Cu(I)-catalyzed [C + NC + CC] reaction favored formation of the corresponding *exo*-cycloadducts **5**/**ent-5**. The relative stereochemistry of the cycloadducts was supported by NOE data (Supporting Information). In the method's original manifestation using enolizable aldehydes, all three [C + NC + CC] components could be combined at once since the enhanced α-acidity of the *N*-acylsultam resulted in rapid conversion of the transient Schiff base to a metallo-azomethine ylide. However, with the heteroaromatic aldehydes **1** described herein, it was found that preforming the Schiff base was optimal for the cycloaddition.

Oppolzer's camphorsultam, which is readily available as either antipode, directed the absolute facial selectivity of the cycloaddition and provided a convenient handle for purification, analysis, and subsequent chemistry. Since the camphorsultam auxiliary is enantiomerically pure, the cycloadducts and derivatives thereof are also enantiomerically pure. This was confirmed in one case using chiral HPLC (Supporting Information). The *N*-acylsultam also provided a convenient synthetic handle for derivatization as exemplified by conversion of the cycloadducts to their corresponding methyl esters and alcohols as shown. By using this methodology, a total of 48 structurally distinct fragments (**6a−f**, **7a−f**, **8a−f**, **9a−f**, **ent-6a-f**, **ent-7a-f**, **ent-8a-f**, and **ent-9a-f**) may be synthesized in just three steps from readily available starting materials.

The chemistry described herein is able to generate unique collections of homochiral pyrrolidines. Our strategy is distinguished from prior approaches to pyrrolidine fragments in that the diversity is installed up front through the use of a robust reaction that is general and tolerant of ancillary functionality. From a fragment design standpoint, we chose synthetic components that would generate cycloadducts with properties that are consistent with known desirable fragment properties (such as Ro3). In order to profile the library, we generated a virtual matrix of the 48 fragments using AbbVie's internal design platform and calculated both physicochemical and shape-based properties. This three-point of diversity library arose via the cycloaddition of six heterocyclic aldehydes (**1**, hArCHO) with both enantiomers of the Oppolzer sultam-derived glycyl amines (**2**/**ent-2**), which generates a reactive azomethine ylide that reacts with a single dipolarophile (acrylonitrile). Depending on the catalyst employed and the two different final auxiliary cleavage steps, 48 unique fragment products are possible. Note that acrylonitrile was employed as it is a highly activated dipolarophile giving either the *endo* or *exo* cycloadduct selectively. The carbonitriles produced can act as good hydrogen bond acceptors for fragment binding and/or offer a flexible synthetic handle that can be transformed into a variety of functionality for further fragment optimization. The added flexibility of controlling *endo/exo* facial selectivity is particularly useful as it allows for a much more robust sampling of vector space via position 4 of the pyrrolidine.

Overall, the diversity of this set of fragments from a 2D standpoint (ECFP-6 fingerprints with 10% belief) is rather limited giving just two clusters. However, when a much more comprehensive set of chemical descriptors are used, such as the 600 or so used for t-SNE (t-directional stochastic neighbor embedding) clustering, differentiation between fragments is apparent and significant.[18] Note that t-SNE allows for the visualization of high-dimensional data via dimensionality reduction into 2D, represented as dim1 (x) and dim2 (y) in the diversity plot shown in Figure 1. The algorithm reduces

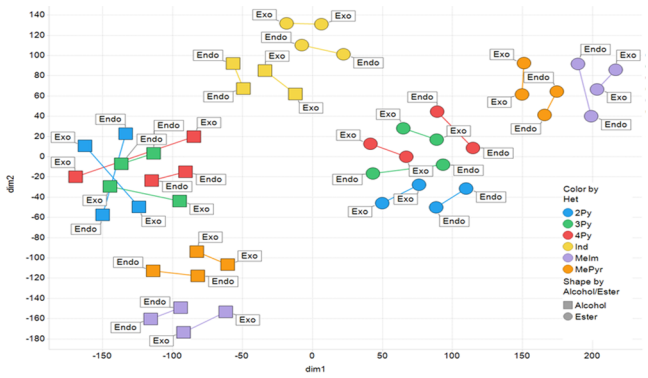

Figure 1. t-SNE clustering of 48 fragments with enantiomeric pairs connected by a line, colored by nature of the heteroaromatic ring system and labeled based on relative stereochemistry.

DOI: 10.1021/acsmedchemlett.9b00070
ACS Med. Chem. Lett. 2019, 10, 811−815

dimensionality and preserves neighborhood distance such that adjacent fragments on the plot are the most similar by virtue of multidirectional space. This manifests in the diversity plot as each of the enantiomeric pairs are close neighbors and connected by a line. Many of the pairs are in the same cluster or are connected to a cluster directly adjacent to its enantiomer. Here, you can clearly see that all three regioisomeric pyridine-containing heterocycles (4Py, 3Py, and 2Py) are clustered together with two distinct clusters differentiated by the final cleavage, providing either the alcohol or ester. This trend is also evident for the two sets of five-membered heterocycles, the methyl pyrazoles (MePyr) and methylimidadzoles (MeIm). The indoles (Ind), however, occupy a unique area of diversity space with both the alcohols and esters within close proximity when embedded in two-dimension. As such, tSNE is a very efficient method of diverging similarity of fragments that may have convergent 2D similarity.

Assessment of the physicochemical property profiles of these fragments was achieved by calculating numerous physicochemical properties and visualizing in Spotfire (Figure 2). Overall

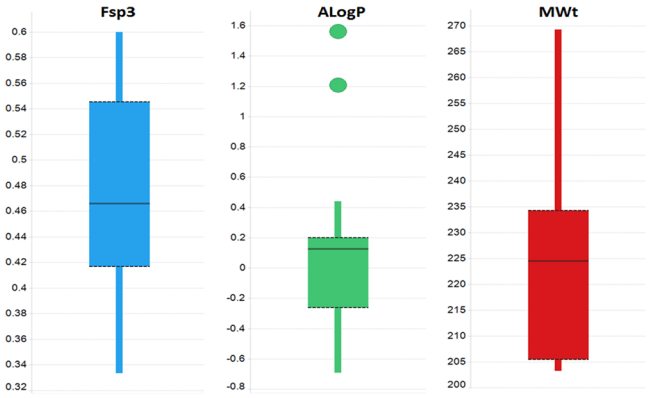

Figure 2. Physicochemical property distributions of the 48 fragments.

these fragments exhibited good physicochemical properties consistent with the desired overall fragment properties of the AbbVie fragment collection, having relatively low lipophilicity (average AlogP = 0.12) and high levels of saturation (average Fsp^3 = 0.47). Note that in general the molecular weight (average MWt = 224.6) of these fragments is at the upper acceptable range for fragments, reflecting the overall increased chemical complexity of these pyrrolidines.

In order to profile the 3D character of these fragments, we looked at two established methods of calculating and defining shape.[19,20] We employed both the normalized principal moments of inertia (NPR1 and NPR2) and plane of best fit (PBF) score to define the three-dimensionality of the fragments. The sum of the NPRs (Σ NPR1 + NPR2) and the PBF scores were calculated, as described by Firth et al., using AbbVie's internal informatics platform and the data visualized in Spotfire (Figure 3). Following the guidelines suggested by Firth, 3D space is defined as Σ NPR1 + NPR2 ≥ 1.07 and PBF score ≥ 0.6. Clearly, all but one of the fragments occupies 3D space (top right quadrant) by virtue of these two shape-based descriptors. As a comparison, we also calculated Σ NPR1 + NPR2 and PBF scores for one of AbbVie's fragment libraries and overlaid the results with the library of 48 pyrrolidines (Figure 4). Clearly these pyrrolidine fragments sit well within 3D space and occupy unique regions based (prospectively) on the nature of the heteroaryl aldehydes,

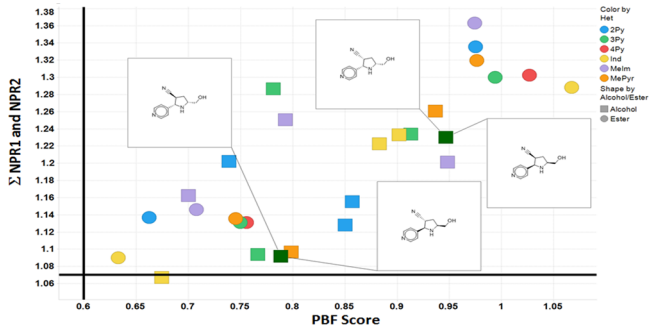

Figure 3. Plot of the sum of the normalized PMI versus PBF scores for all 48 fragments. Enantiomeric pairs of two sets of regioisomers derived from isonicotinaldehyde are highlighted. Fragments are colored by the type of heteroaryl aldehyde used with the final transformation into alcohol or ester distinguished by marker shape.

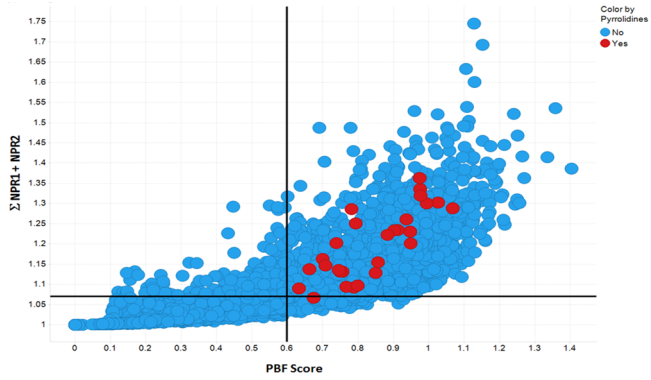

Figure 4. Plot of the sum of the normalized PMI versus PBF scores for the pyrrolidines compared with an internal AbbVie fragment library. Red circles are the 48 pyrrolidine fragments, and blue circles are 4000 fragments from AbbVie's collection.

facial selectivity of the 1,3-dipolar cycloaddition (*endo* vs *exo*), and the final auxiliary cleavage, which delivers either the ester or alcohol. In order to demonstrate the scope and extent of vector coverage in 3D space for these pyrrolidines, we overlaid the conformations of each of the pyrrolidines generated for calculating PBF and PMI relative to the unsubstituted central pyrrolidine scaffold (Figure 5).

Just considering the relative distribution of the carbonitrile vector alone, there is considerable coverage in 3D space relative to the common central pyrrolidine scaffold. In other words, the combination of six aldehydes with acrylonitrile, in the context of this metal-catalyzed asymmetric 1,3-dipolar cycloaddition cascade, can generate an array of 48 unique fragments that occupy, and thereby sample, unique regions of molecular space, both from a shape and multiparametric perspective. By developing chemistry, as described, which generates stereochemically enriched fragments, it is possible to synthesize arrays with divergent 3D similarity, despite possessing convergent 2D similarity. This has implications with respect to the added overall complexity of chemical space, as current estimates do not take into consideration 3D, let alone the multidimensional descriptors of chemical space. Clearly in this regard, the more chiral centers one adds to a fragment/scaffold, the greater the chemical complexity of the space that chemical matter occupies. Whether designing fragments with enhanced 3D molecular complexity improves the probability of a binding event remains to be seen with

DOI: 10.1021/acsmedchemlett.9b00070
ACS Med. Chem. Lett. 2019, 10, 811−815

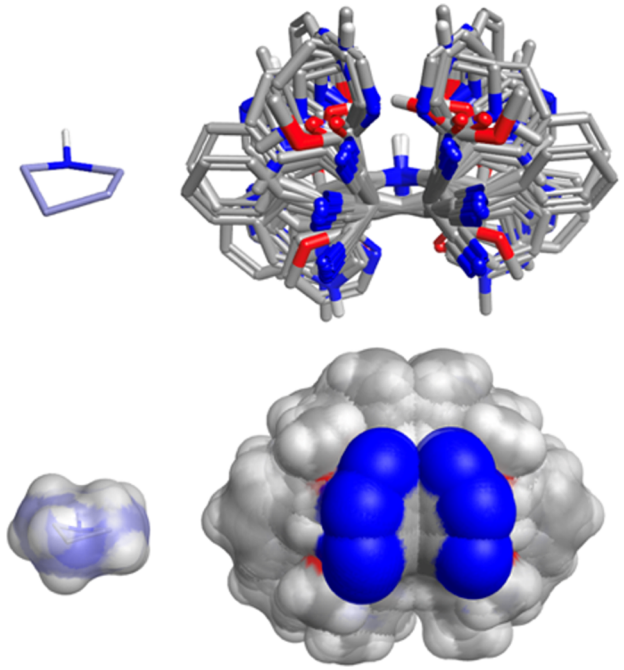

Figure 5. Overlay of all 48 pyrrolidines showing relative position of vectors from the central pyrrolidine core. For reference, the pyrrolidine core of one structure is shown on the left.

regard to the fragment screening campaigns at AbbVie. Note, however, that Astex have shown that the 3D character of fragments has an overall negative effect on the hit rates of their fragment screens.[21] By comparing the deviation from planarity DFP descriptor (as a surrogate of 3D) distribution of the fragment screening deck vs that of fragment hits, in all cases the percentage of 3D hits was less than the original screening deck. It is important to note though that although there was an overall drop in the percentage of hits with high degrees of DFP, for PPI targets over 10% of the fragment hits had a high degree of 3D character (DFP > 0.5) with a DFP distribution similar to the screening library. Clearly the right balance of molecular complexity in both two- and three-dimensions for fragments is very important with respect to designing fragment libraries that efficiently sample chemical space.

In this Letter, we have demonstrated how the asymmetric [C + NC + CC] cycloaddition reaction can be used to generate enantiomerically pure pyrrolidine fragments with a high degree of both saturation and shape (3D) diversity. Coverage of 3D molecular and functional group space may be expanded by varying the structures of the aldehyde (C) and alkene (CC)[16,17] components, as well as the chemical transformation applied to the acyl sultam moiety (derived from the NC component). The resulting methodology may be used to add significant shape-based diversity to fragment collections.

■ ASSOCIATED CONTENT

Supporting Information

The Supporting Information is available free of charge on the ACS Publications website at DOI: 10.1021/acsmedchemlett.9b00070.

Experimental procedures and characterization data for all new compounds (PDF)

■ AUTHOR INFORMATION

Corresponding Authors

*(P.G.) E-mail: ppg@wsu.edu. Phone: (+1) 509-335-7620.
*(P.B.C.) E-mail: phil.cox@abbvie.com. Phone: (+1) 847-938-5422.

ORCID

Philip Garner: 0000-0002-6503-9550

Author Contributions

The manuscript was written through contributions of all authors. All authors have given approval to the final version of the manuscript.

Notes

The authors declare the following competing financial interest(s): P.C. and P.E. are employees of AbbVie, and U.R. was an employee during the time of this study. The design, study content, and financial support for the study were provided by AbbVie. AbbVie participated in the interpretation of data, review, and approval of the publication. Note that P.G. has received research funding and speaker fees from AbbVie. N.H. is an employee of Washington State University and has nothing to disclose.

■ ACKNOWLEDGMENTS

The authors wish to thank Drs. Stevan Djuric and Anil Vasudevan of AbbVie for continued support of this project. Support from the Research Informatics group at AbbVie (Rishi Gupta and Abhik Seal) is also greatly appreciated. Thanks also to Dr. Gregory Helms (WSU) for his technical assistance with the NMR characterizations.

■ ABBREVIATIONS

FBDD, fragment-based drug discovery; 3D, three-dimensional; TLC, thin layer chromatography; PMI, principal moments of inertia; NPR, normalized principal moments of inertia; PBF, plane of best fit; AlogP, calculated atom log partition coefficient (octanol/water); Fsp3, fraction of sp^3 carbons/total number of carbons; MW, molecular weight; Py, pyridine; Ind, indole; MeIm, methyl imidazole; MePy, methyl pyrazole

■ REFERENCES

(1) Lamoree, B.; Hubbard, R. Current Perspectives in Fragment-Based Lead Discovery (FBLD). *Essays Biochem.* **2017**, *61*, 453−464 and references therein .

(2) Lovering, F.; Bikker, J.; Humblet, C. Escape from Flatland: Increasing Saturation as an Approach to Improving Clinical Success. *J. Med. Chem.* **2009**, *21*, 6752−6756.

(3) Vitaku, E.; Smith, D. T.; Njardarson, J. T. Analysis of the Structural Diversity, Substitution Patterns and Frequency of Nitrogen Heterocycles among US FDA Approved Pharmaceuticals. *J. Med. Chem.* **2014**, *57*, 10257−10274.

(4) Hashimoto, T.; Maruoka, L. Recent Advances of Catalytic Asymmetric 1,3-Dipolar Cycloadditions. *Chem. Rev.* **2015**, *115*, 5366−5412.

(5) Adrio, J.; Carretero, J. C. Recent Advances in the Catalytic Asymmetric 1,3-dipolar Cycloaddition of Azomethine Ylides. *Chem. Commun.* **2014**, *50*, 12434−12446.

(6) Longmire, J. M.; Wang, B.; Zhang, Z. Highly Enantioselective Ag(I)-Catalyzed [3 + 2] Cycloaddition of Azomethine Ylides. *J. Am. Chem. Soc.* **2002**, *124*, 13400−13401.

(7) Pfaltz, A.; Stohler, R.; Wahl, F. Enantio- and Diastereoselective [3 + 2] Cycloadditions of Azomethine Ylides with Ag(I)-Phosphinooxazoline Catalysts. *Synthesis* **2005**, 1431−1436.

DOI: 10.1021/acsmedchemlett.9b00070
ACS Med. Chem. Lett. 2019, 10, 811−815

(8) Zeng, W.; Zhou, Y. G. Bifunctional AgOAc-catalyzed Asymmetric [3 + 2] Cycloaddition of Azomethine Ylides. *Org. Lett.* **2005**, *7*, 5055−5058.
(9) Cabrera, S.; Arrayás, R. G.; Martín-Matute, B.; Cossío, F. T.; Carretero, J. C. Cu^{I}−Fesulphos Complexes: Efficient Chiral Catalysts for Asymmetric 1,3-Dipolar Cycloaddition of Azomethine Ylides. *Tetrahedron* **2007**, *63*, 6587−6602.
(10) Agbodjan, A. A.; Cooley, B. E.; Copley, R. C. B.; Corfield, J. A.; Flanagan, R. C.; Glover, B. N.; Guidetti, R.; Haigh, D.; Howes, P. D.; Jackson, M. M.; Matsuoka, R. T.; Medhurst, K. J.; Millar, A.; Sharp, M. J.; Slater, M. J.; Toczko, J. F.; Xie, S. Asymmetric Synthesis of an N-Acylpyrrolidine for Inhibition of HCV Polymerase. *J. Org. Chem.* **2008**, *73*, 3094−3102.
(11) Wang, C.-J.; Liang, G.; Xue, Z.-Y.; Gao, F. Highly Enantioselective 1,3-Dipolar Cycloaddition of Azomethine Ylides Catalyzed by Copper(I)/TF-BiphamPhos Complexes. *J. Am. Chem. Soc.* **2008**, *130*, 17250−17251.
(12) Padilla, S.; Tejero, R.; Adrio, J.; Carretero, J. C. N-(2-Pyridylmethyl)imines as Azomethine Precursors in Catalytic Asymmetric [3 + 2] Cycloadditions. *Org. Lett.* **2010**, *12*, 5608−5611.
(13) Yamashita, Y.; Imaizumi, T.; Kobayashi, S. Chiral Silver Amide Catalyst for the [3 + 2] Cycloaddition of 2-Amino Esters to Olefins. *Angew. Chem., Int. Ed.* **2011**, *50*, 4893−4896.
(14) Chaulagain, M. R.; Felten, A. E.; Gilbert, K.; Aron, Z. Diastereo-and Enantioselective Three-component Coupling Approach to Highly Substituted Pyrrolidines. *J. Org. Chem.* **2013**, *78*, 9471−9476.
(15) Xiong, Y.; Du, Z.; Chen, H.; Yang, Z.; Tan, Q.; Zhang, C.; Zhu, L.; Lan, Y.; Zhang, M. Well-Designed Phosphine-Urea Ligand for Highly Diastereo- and Enantioselective 1,3-Dipolar Cycloaddition of Methacrylonitrile: A Combined Experimental and Theoretical Study. *J. Am. Chem. Soc.* **2019**, *141*, 961−971.
(16) Garner, P.; Kaniskan, H. Ü.; Hu, J.; Youngs, W. J.; Panzner, M. Asymmetric Multicomponent [C + NC + CC] Synthesis of Highly Functionalized Pyrrolidines Catalyzed by Silver(I). *Org. Lett.* **2006**, *8*, 3647−3650.
(17) Garner, P.; Hu, J.; Parker, C. G.; Youngs, W. J.; Medvetz, D. The Cu^{I}-catalyzed *Exo*-Selective Asymmetric Multicomponent [C + NC + CC] Coupling Reaction. *Tetrahedron Lett.* **2007**, *48*, 3867−3870.
(18) van der Maarten, L. J. P. Accelerating t-SNE using Tree-Based Algorithms. *Journal of Machine Learning Research.* **2014**, *15*, 3221−3245.
(19) Muchmore, S. W.; Debe, D. A.; Metz, J. T.; Brown, S. P.; Martin, Y. C.; Hajduk, P. J. Application of Belief Theory to Similarity Data Fusion for Use in Analog Searching and Lead Hopping. *J. Chem. Inf. Model.* **2008**, *48*, 941−948.
(20) Firth, N. C.; Brown, N.; Blaff, J. Plane of Best Fit: A Novel Method to Characterize the Three-Dimensionality of Molecules. *J. Chem. Inf. Model.* **2012**, *10*, 2516−2525.
(21) Hall, R. J.; Mortenson, P. N.; Murray, C. W. Efficient exploration of chemical space by fragment-based screening. *Prog. Biophys. Mol. Biol.* **2014**, *10*, 82−91.

DOI: 10.1021/acsmedchemlett.9b00070
ACS Med. Chem. Lett. 2019, 10, 811−815